Characterizing the population of pulsars in the Galactic bulge with the Fermi Large Area Telescope

ArXiv:1705.00009 Submitted to ApJ

Mattia Di Mauro

Eric Charles, Matthew Wood

On behalf of the Fermi-LAT Collaboration

Stanford University

SLAC NATIONAL ACCELERATOR LABORATORY

TeVPA 2017, August 7th.

The GeV Excess in the Galactic Center

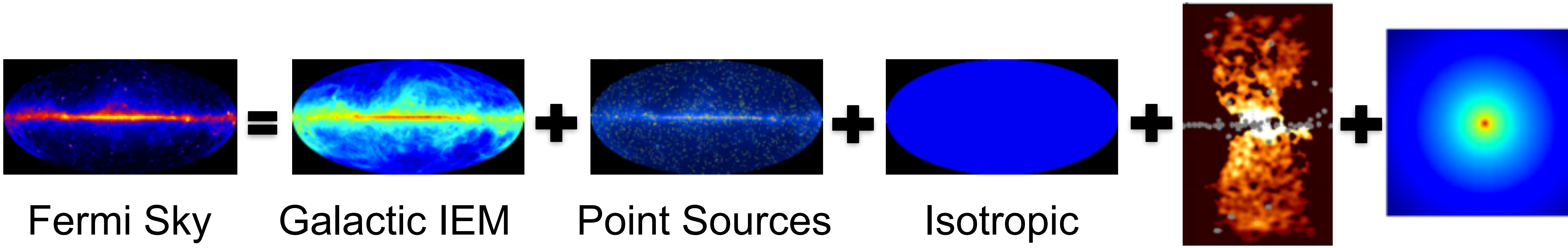

Fermi Sky = Galactic IEM + Point Sources + Isotropic + Fermi Bubbles + DM

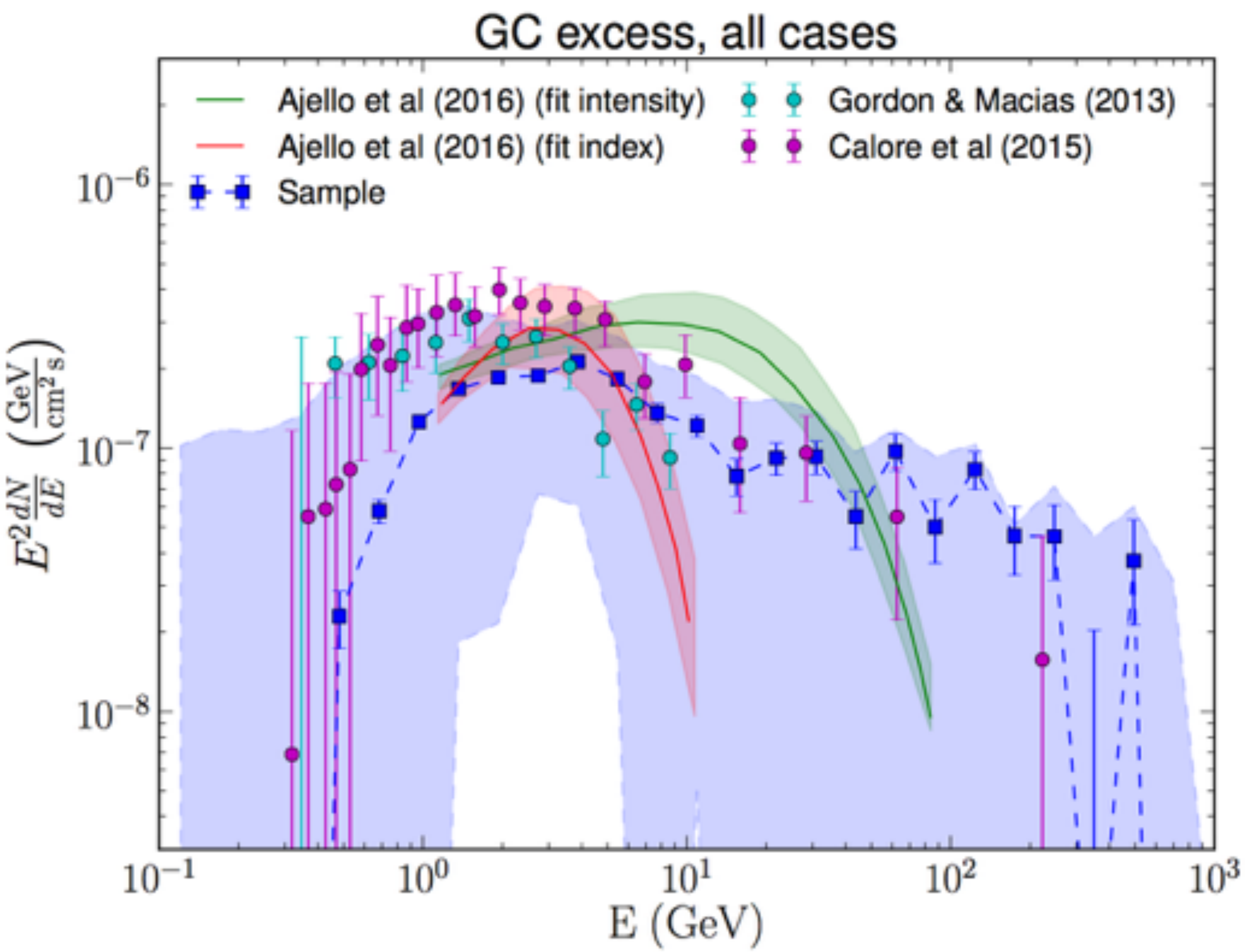

Ajello et al. 2017

Shape and intensity of the GeV excess depends on the choice of:

- Source catalog
- Fermi Bubble template
- Inverse Compton+ π^0 +bremsstrahlung (IEM).
- Source spatial distribution

Pulsar interpretation

- **Bartels et al. (2015) and Lee et al. (2015):** population of unresolved sources distributed in the Galactic bulge of our Galaxy → Pulsars.
- The spatial distribution, total γ-ray emission and energy spectrum of this unresolved emission of pulsars is compatible with the GeV excess.
- A fraction of these faint sources should be detected with future Fermi-LAT catalogs (Bartels et al. 2015 and Hooper et al. 2014).

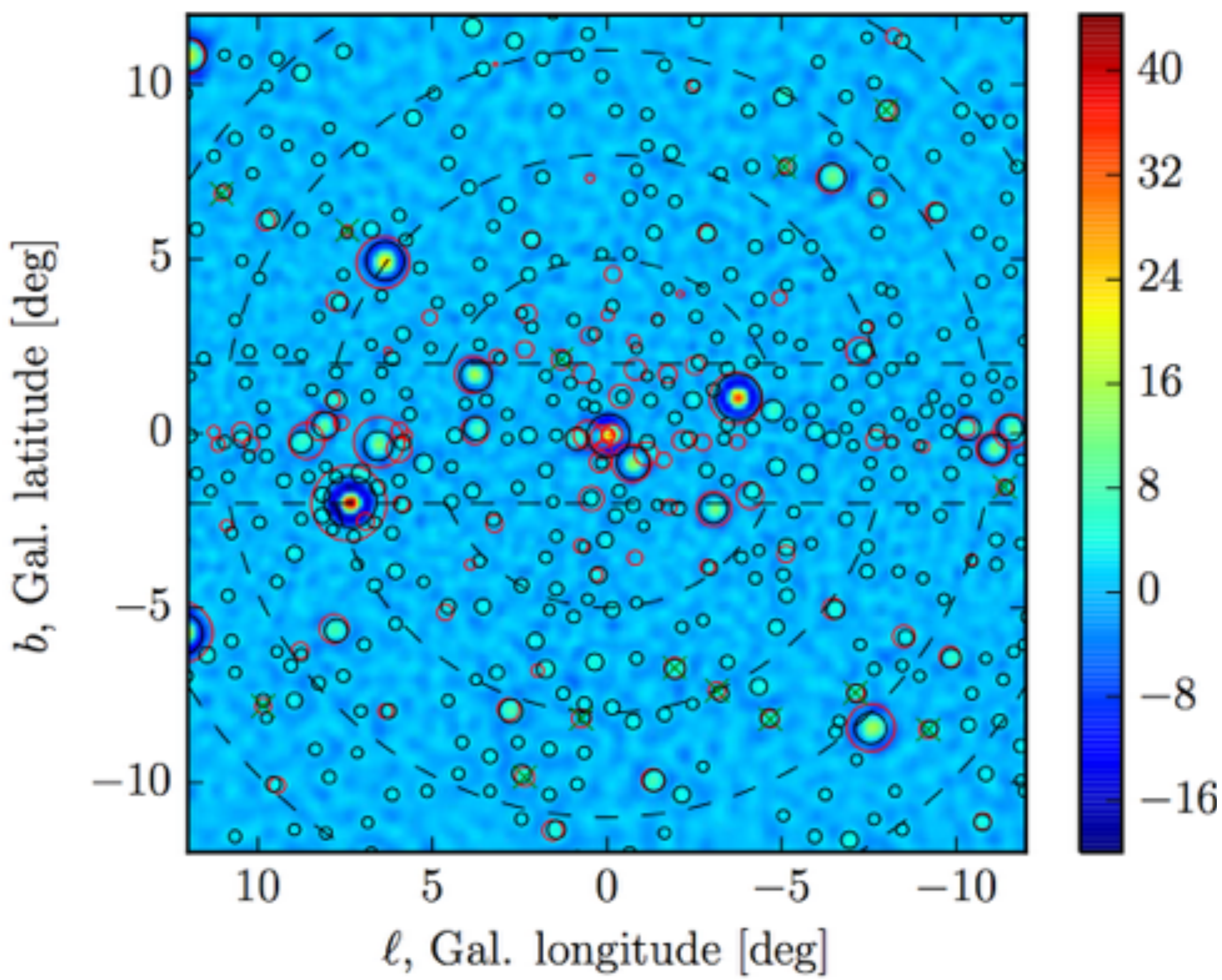

Bartels et al. 2015

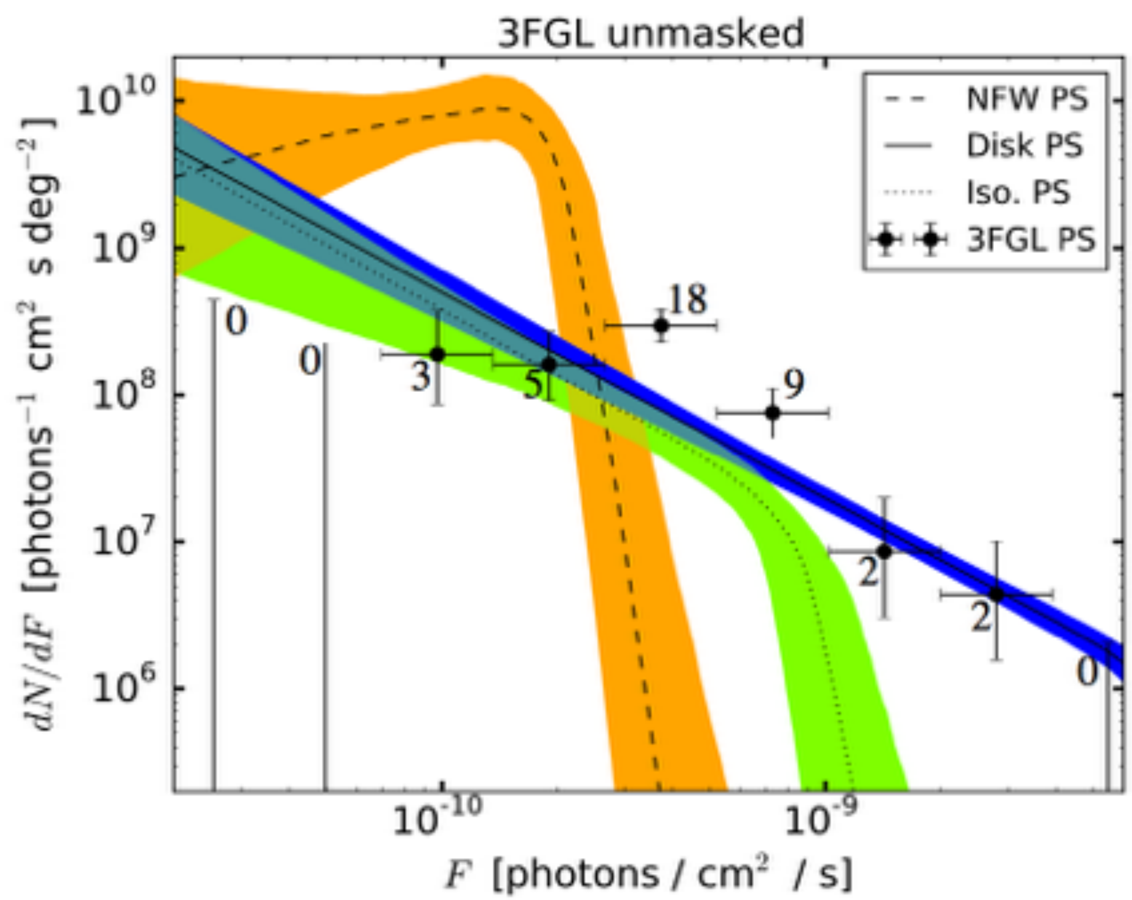

Lee et al. 2015

Goals and analysis details

GOALS

- Derive a catalog of sources with two different IEMs.
- Select among those sources PSR candidates.
- Using the spatial distribution and ray flux of our PSR candidates to characterize the Galactic bulge population of PSRs.
- Test the PSR interpretation of the GC excess versus the DM interpretation.

ANALYSIS DETAILS

- **40x40 deg^2** region centered around the GC.
- **74 months** of Pass 8 SOURCE data with **E=[0.3,500] GeV** energy range.
- We use **two different IEMs that we label OFFICIAL (Off.) and ALTERNATE (Alt.)**

2FIG source list

IEM	N(|b|,|l|<20deg)	3FGL detection rate
Off.	371	189/202
Alt.	381	182/202

- White markers: 3FGL sources.
- Green markers: new sources
- Blue stars: identified PSRs.
- Purple markers: sources belonging to a cluster.

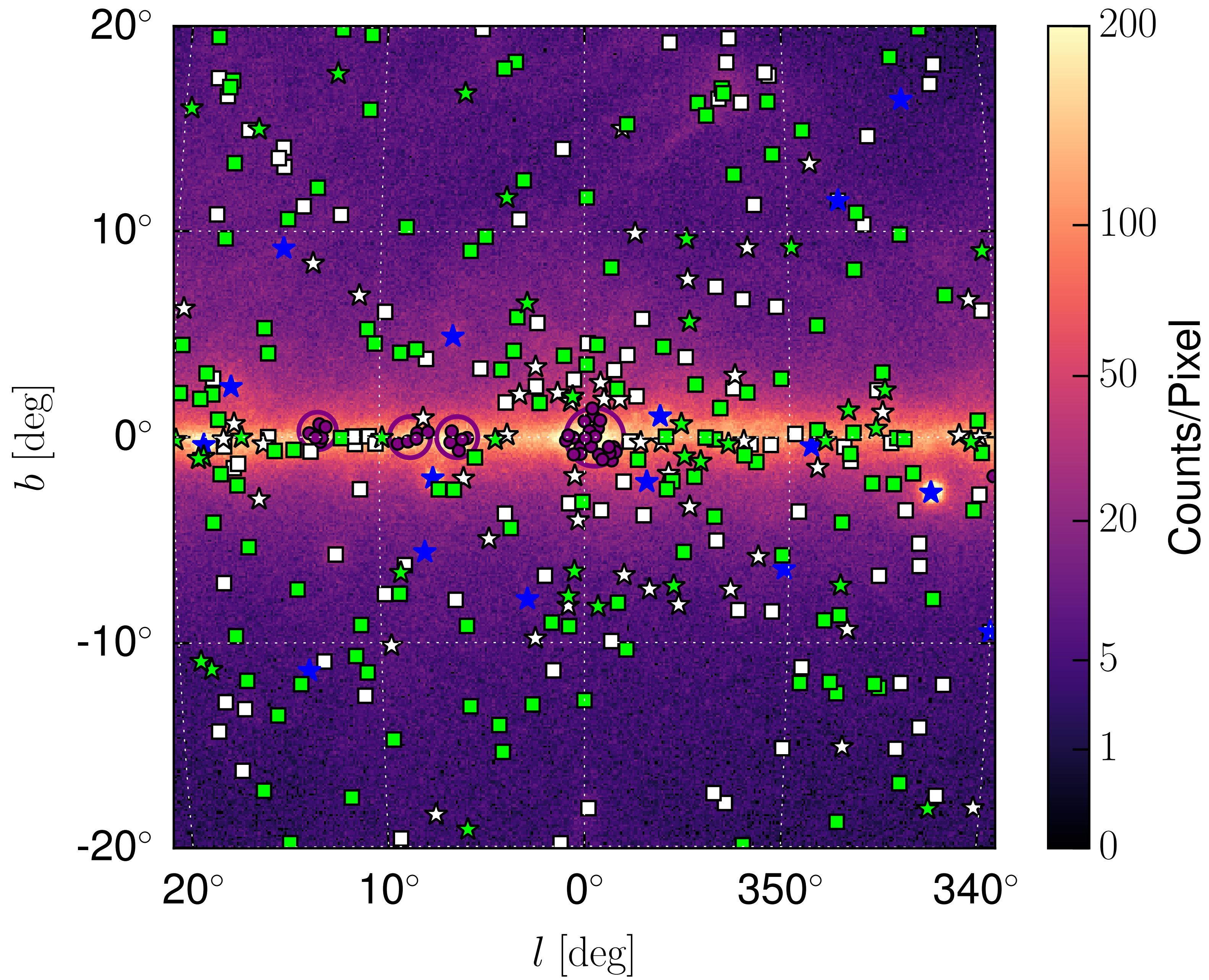

SED OF BLAZARS AND PULSARS IN 3FGL

- 70% of PSRs in the 3FGL have an SED fitted with a PLE: $\mathbf{TS^{PLE}_{curv.}}$
- Our sample: 210 PSRs* and of 3FGL blazars with $\mathbf{TS^{PLE}_{curv}}$>9 (9% of 3FGL blazars).
- **The selection criteria (TS^{PLE}_{curv}>9, Index<2.0 and E_{cutoff}<10GeV): works very well to separate PSRs from blazars.**

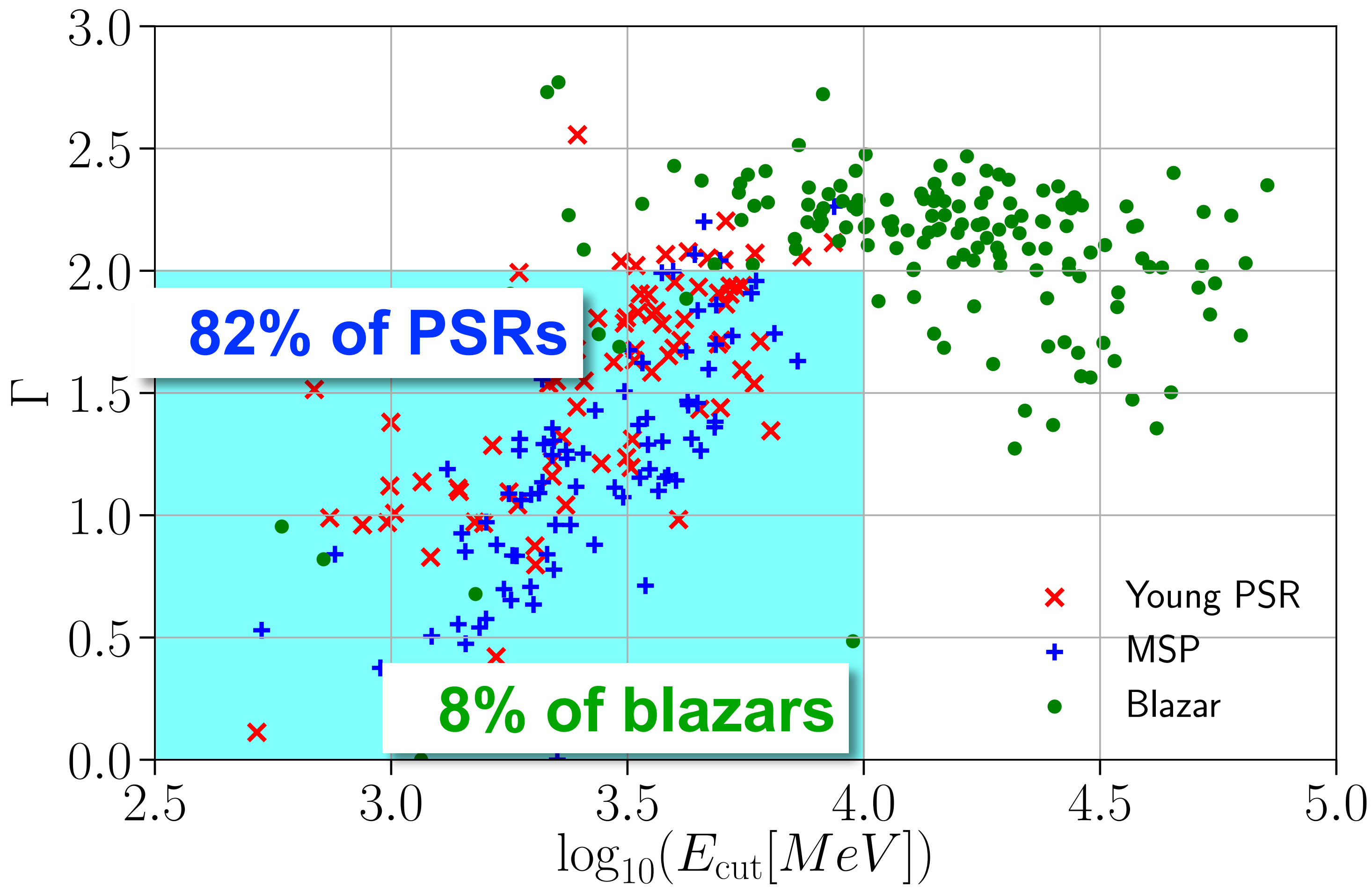

$$\frac{dN}{dE} = K\left(\frac{E}{E_0}\right)^{-\Gamma} \exp\left(-\frac{E}{E_{cut}}\right)^{b}$$

b fixed to 1

*https://confluence.slac.stanford.edu/display/GLAMCOG/Public+List+of+LAT- Detected+Gamma-Ray+Pulsars

PSR Candidates in the GC region

IEM	N_{PSR}	Γ	$\log_{10}(E_{cut}[MeV])$
Off.	86	1.03 ± 0.52	3.28 ± 0.33
Alt.	115	1.05 ± 0.50	3.27 ± 0.31
Alt. ∩ Off. (Off.)	66	1.02 ± 0.52	3.27 ± 0.32
Alt. ∩ Off. (Alt.)	66	1.01 ± 0.51	3.26 ± 0.30
Known PSRs (Off.)	172	1.33 ± 0.54	3.43 ± 0.24
Young PSRs (Off.)	86	1.46 ± 0.53	3.44 ± 0.26
MSPs(Off.)	86	1.20 ± 0.50	3.42 ± 0.23

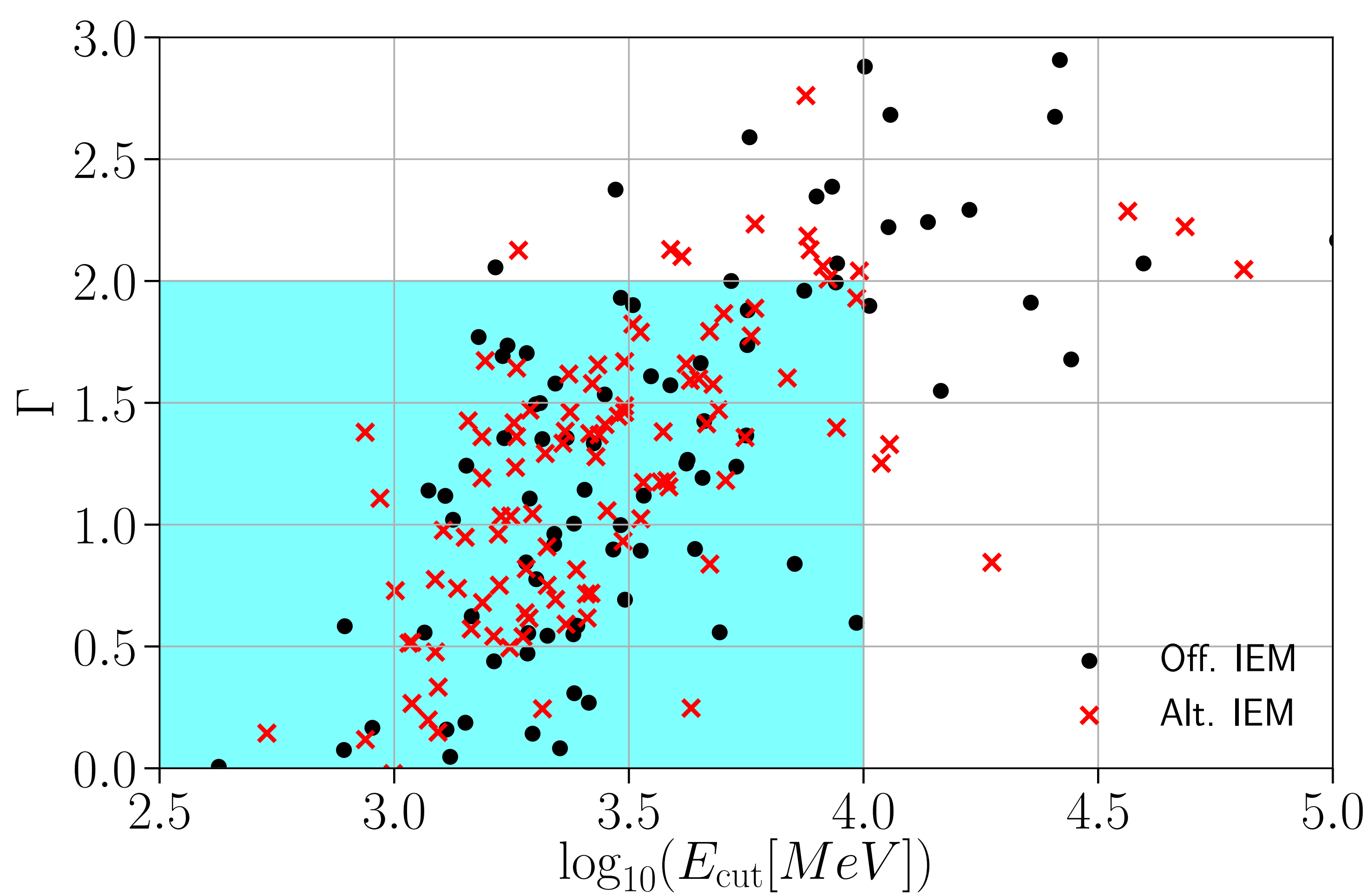

PSR distribution in the GC region

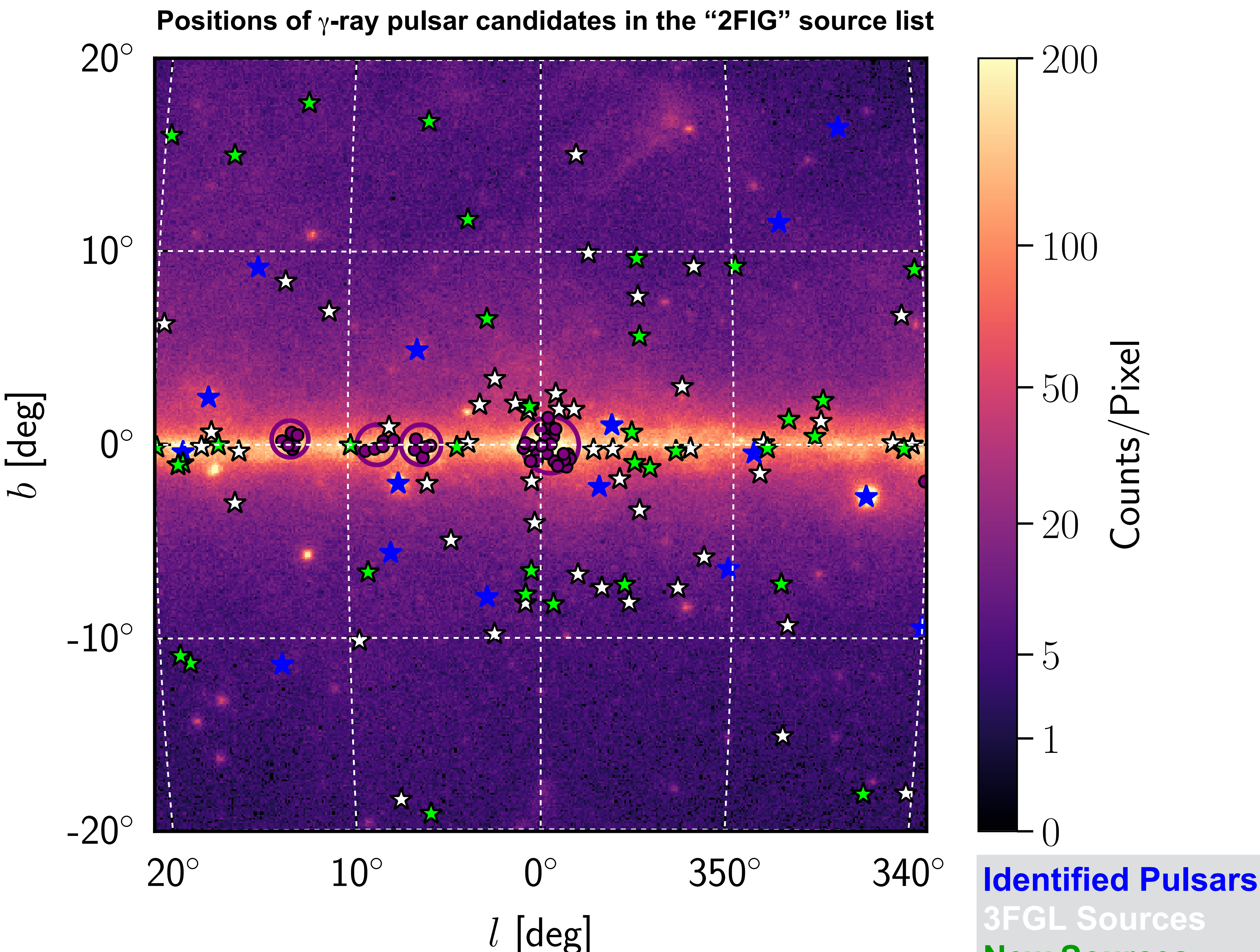

Source population inputs to the simulations

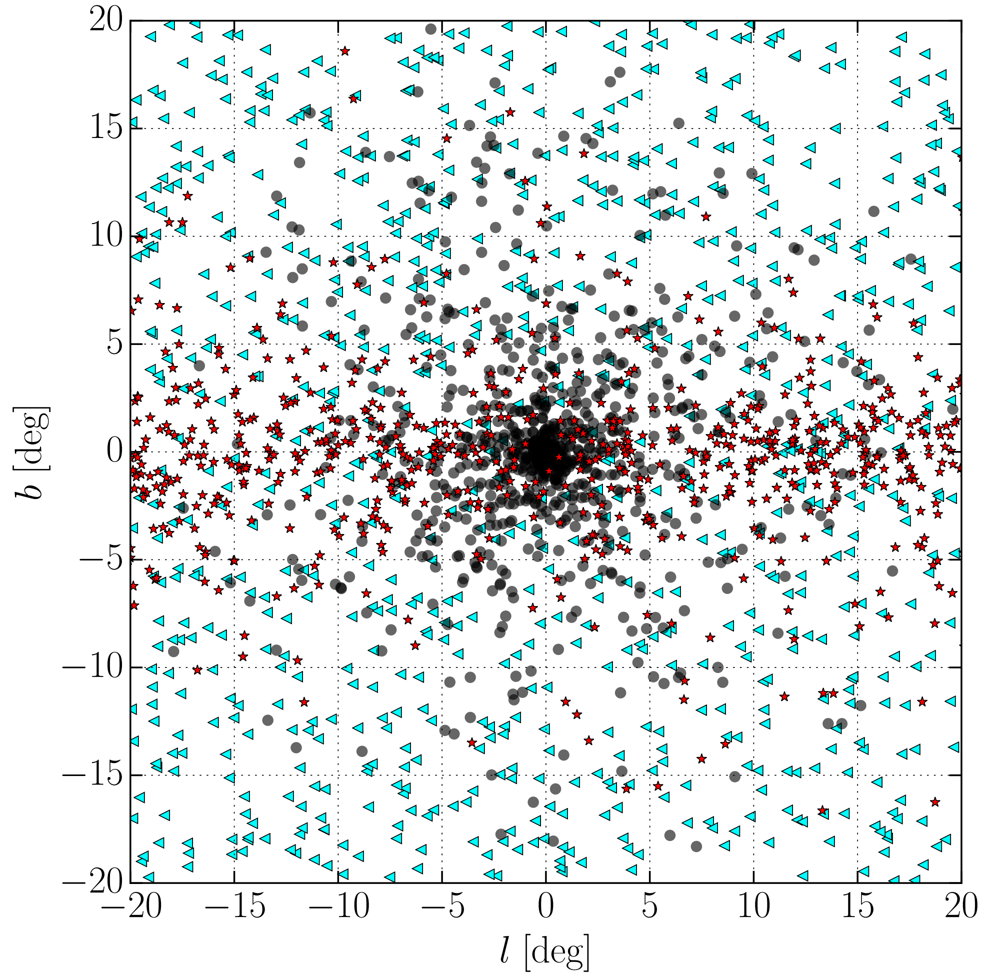

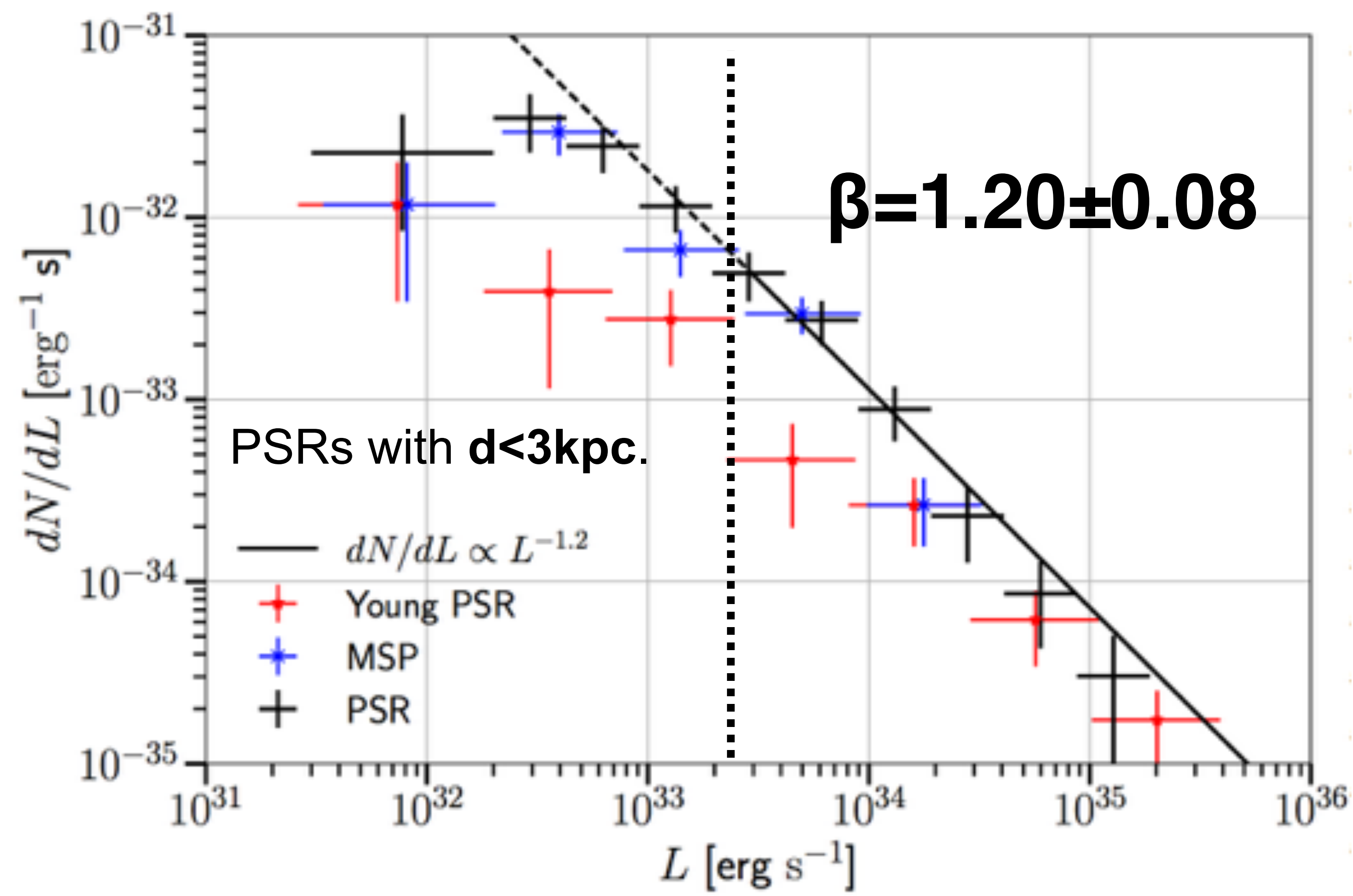

BLAZARS:

A. Isotropically distributed.
B. SED modeled as 3FGL blazars.
C. Intrinsic dN/dS found from the 1FGL.
D. **900 blazars** simulated in the GC region with F>10^{-10} ph/cm^2/s.

DISK PSRs:

A. Luminosity distribution: taken from 3FGL PSRs with **d<3kpc**. β=1.20.
B. Spatial distribution: Lorimer 2004
C. SED parameters: 3FGL PSRs.
D. **[1400,5000] disk PSRs.**

Inner Galaxy PSRs:

A. **dN/dV** ∝ **$r^{-\alpha}$** with a cut at 3 kpc.
B. **[500,2300]** bulge PSRs.

Efficiency for the detection of PSR candidates

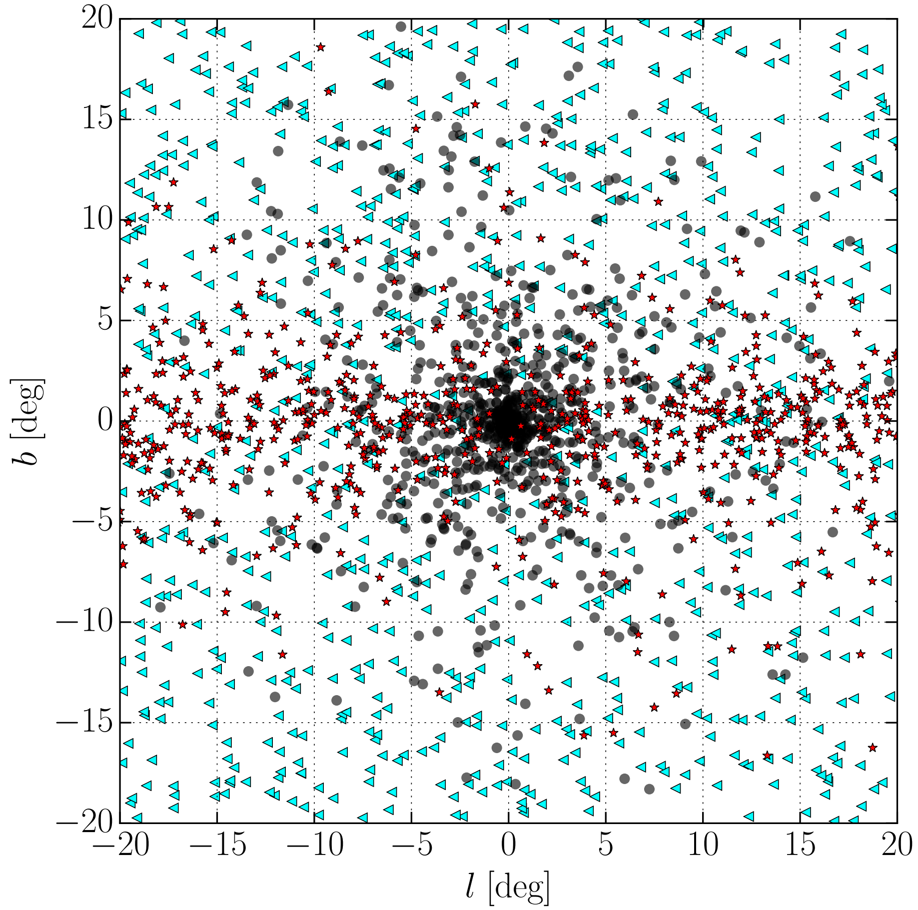

We generate 10 simulations

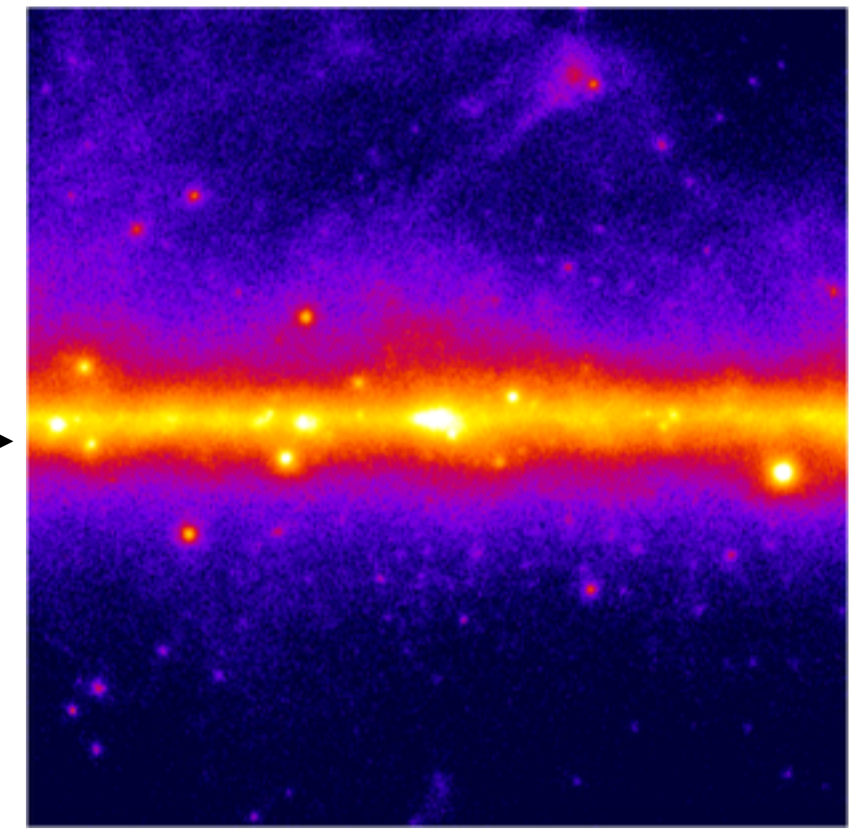

We run the pipeline for the detection of sources and we select PSR-like sources.

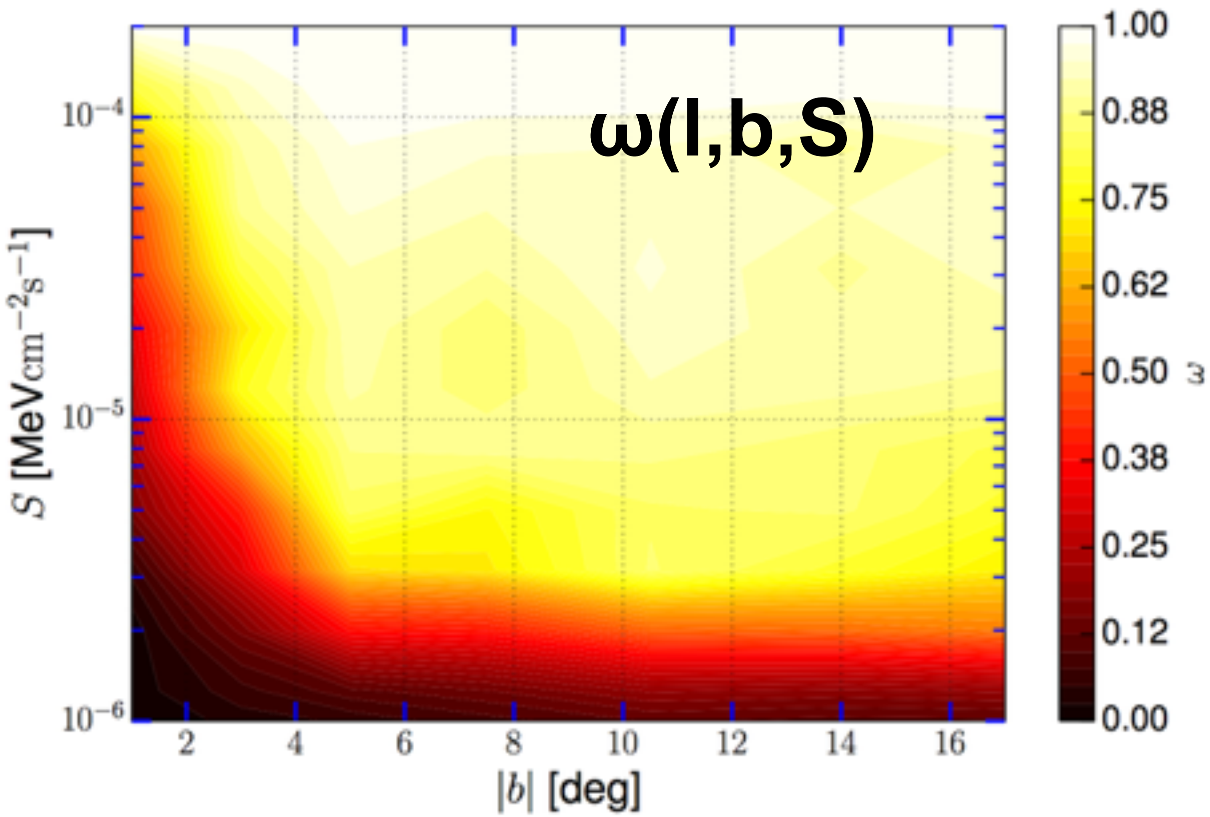

Number of PSRs given by the model

$$N_{\Delta l,\Delta b,\Delta S} = \int_{d\Omega} dl db \int_{l.o.s.} ds \rho(R_{GC}(l,b,s)) \times \int_{L_{min}}^{L_{max}} \frac{dN}{dL} dL$$

Disk	N_{disk}	Lorimer 2004 ρ(r)	$dN/dL \propto L^{-\beta}$
Bulge	N_{bulge}	$dN/dV \propto r^{-\alpha}$	$dN/dL \propto L^{-\beta}$

- Number of detected PSRs from the model: $\mathbf{N_{Model} = N_{\Delta l,\Delta b,\Delta S} \times \omega(l,b,S)}$
- Null hypothesis (H_0): **observed PSRs come from the disk population.**
- TS: **presence of the bulge PSR population.**
- N_{obs} number of 3FGL PSRs and new PSR candidates found in this analysis.
- We apply a Maximum Likelihood analysis (MLA) using Poisson statistics where we compare N_{Model} with N_{obs}.

$$\log(\mathcal{L}) = \sum_{i,j,k} N_{i,j,k}^{obs} \log(N_{i,j,k}^{model}(\lambda)) + N_{i,j,k}^{model}(\lambda) + \mathcal{L}_{prior}$$

Results for the disk+bulge populations

- **H_0 (PSR candidates from the PSR disk):** we need around N_{disk}=20000 disk PSRs with a slope of the luminosity function of β=1.30 for L > 10^{31} erg/s.
- **Disk+Bulge (only N_{bulge} in addition to H0):** this model requires N_{disk}=4000 and N_{bulge}=1400 and β=1.35 (with L > 10^{31} erg/s) and is preferred with at least **7σ** significance wrt H0.
- **α free: α=2.60** consistently with the spatial shape of the GeV excess.
- **The presence of a PSR population in the Galactic bulge is preferred at least at 7σ.**

Latitude Profile of Bulge Sources

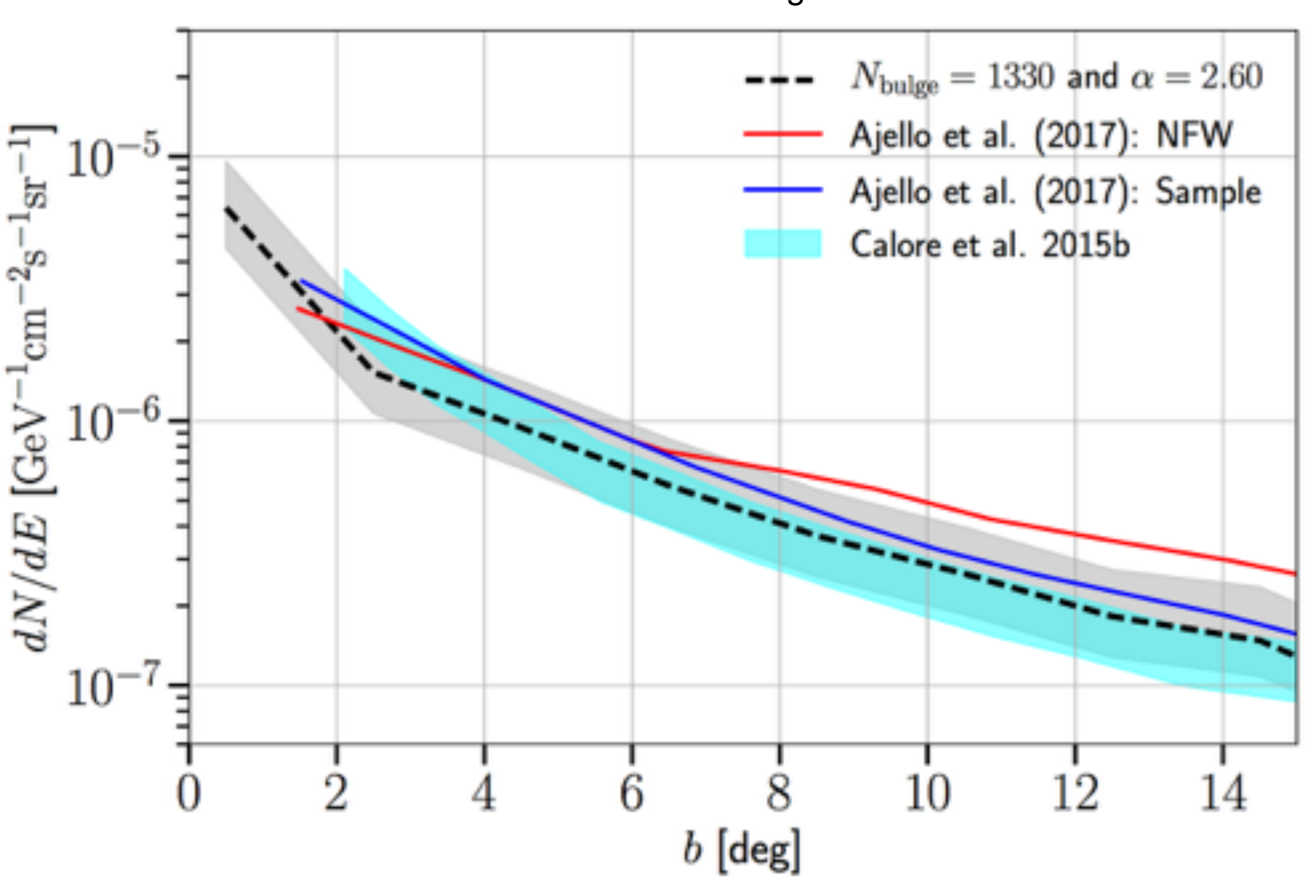

SED of Bulge Sources

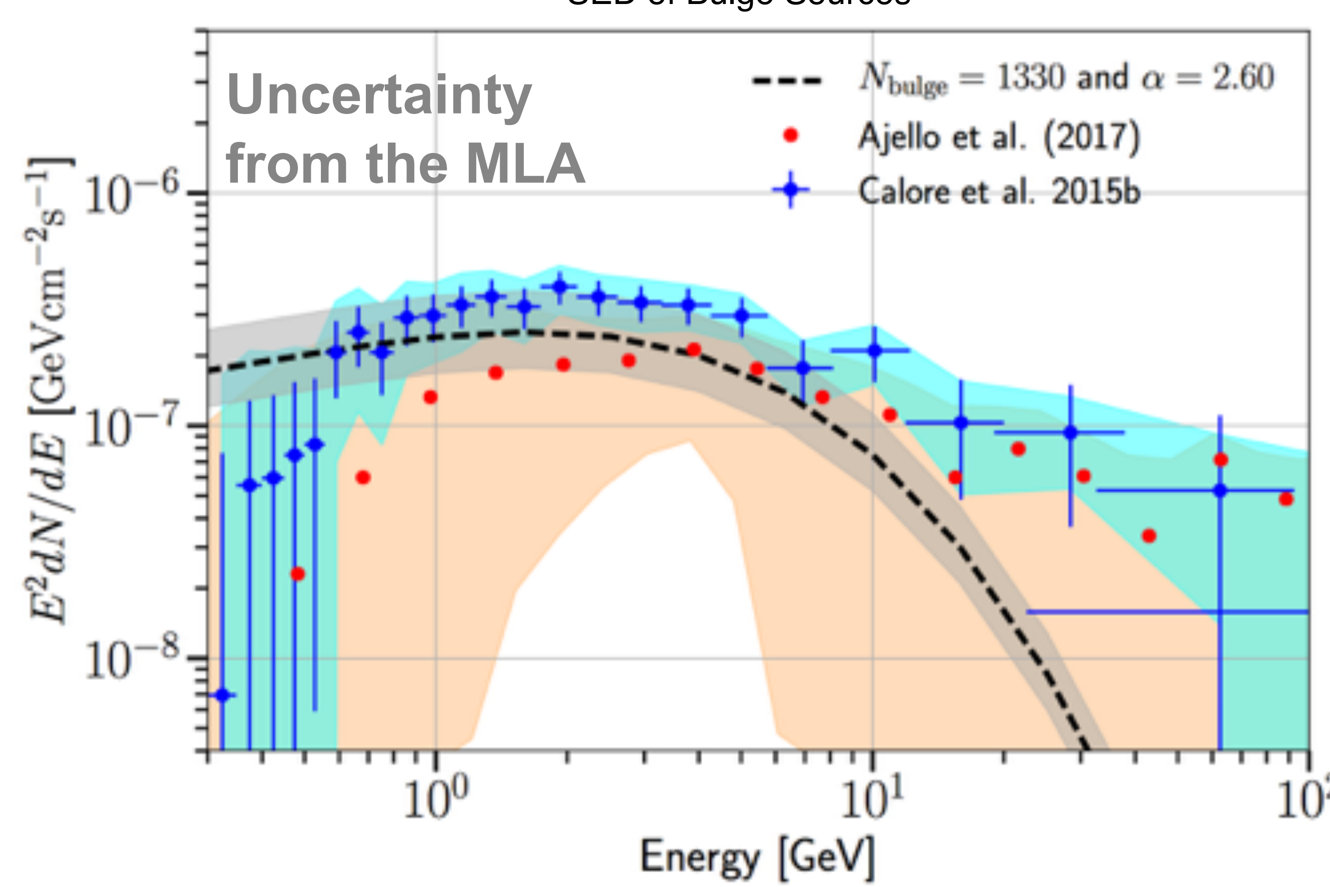

Dark Matter vs PSR in the Galactic bulge

- Considering the GC excess as given by a diffuse template (like DM) as in Ajello et al. 2016.
  - Around 35 **spurious PSR candidates** found within a few degrees from the GC.
- **The DM interpretation of the GeV excess does not reproduce the observed distribution of PSR-like sources!**
- **On the other hand our model with Disk+Bulge PSRs and blazars works very well!**

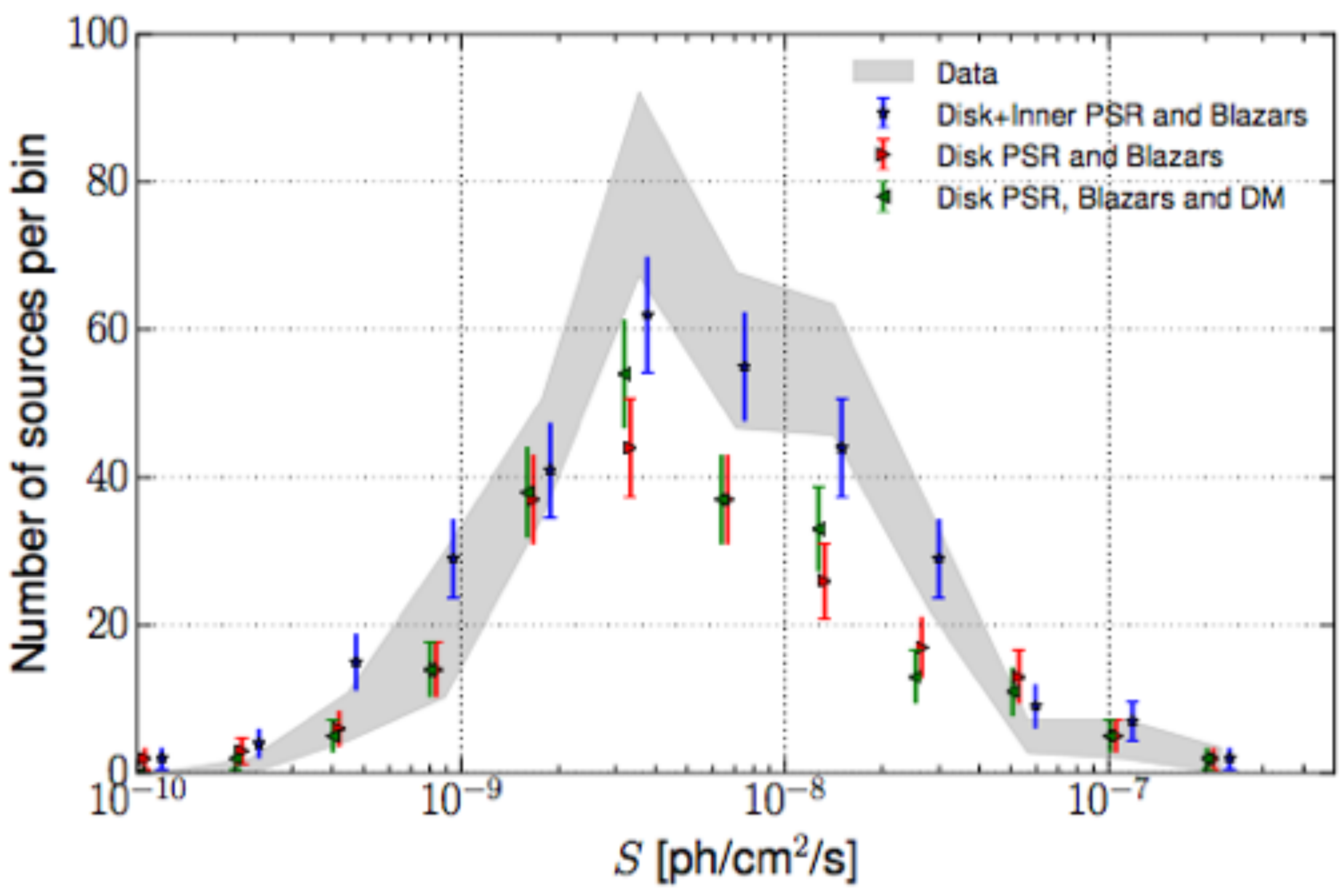

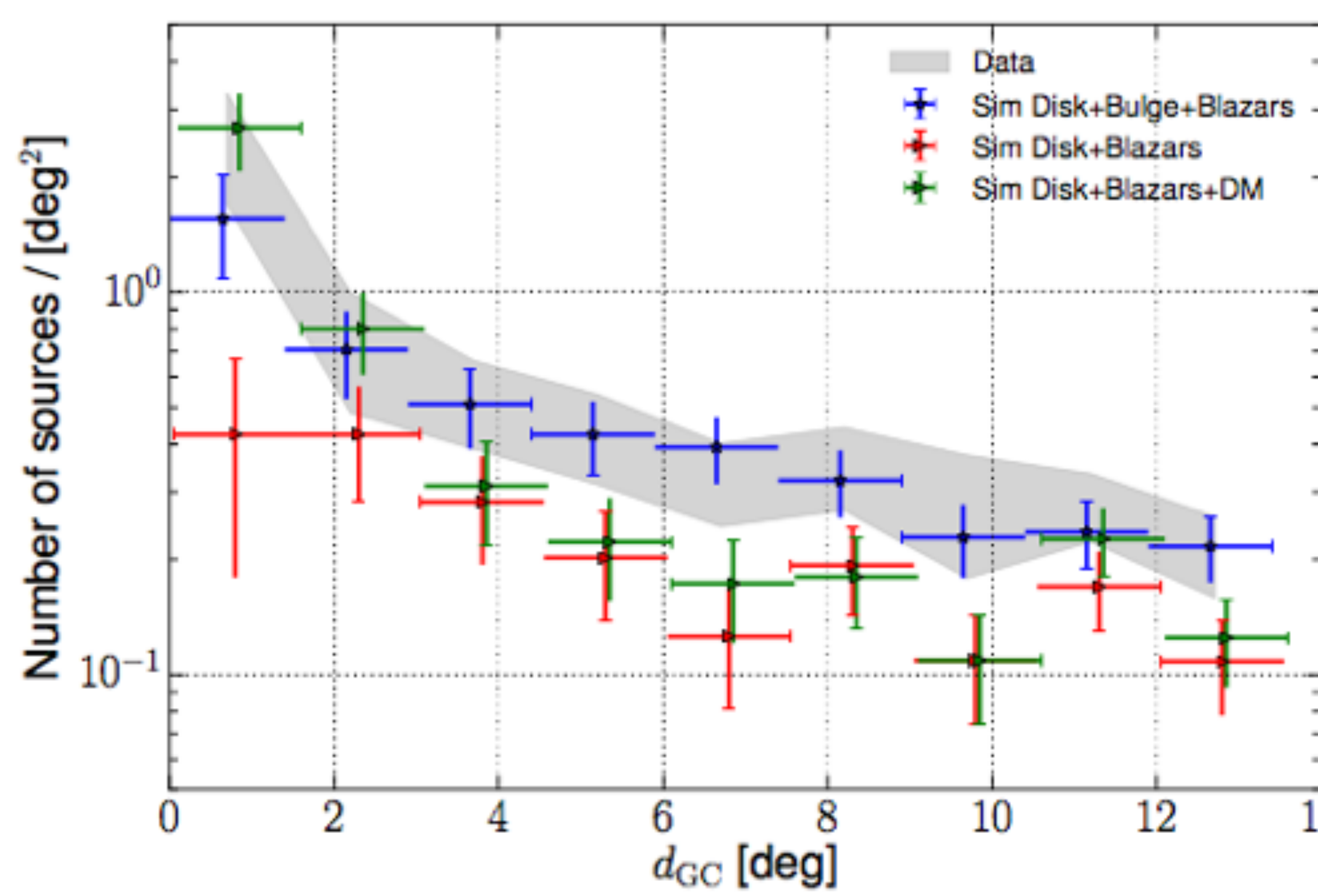

CONCLUSIONS

- Detected almost **400 sources** in 40x40 deg^2 region centered around the GC.
- Using the criteria **TS^{PLE}_{curv}>9, Index<2.0 and E_{cut}<10GeV** we created lists of PSR candidates.
- Found **66 seeds** with PSR-like SEDs, detected with both IEMs, which could be the brightest exemplars of an inner Galaxy PSR population.
- Derived the **efficiency** for the detection of PSR candidates **ω(l,b,S)**
- Using a Maximum Likelihood analysis we have derived that the spatial and flux distribution of our new PSR candidates and 3FGL PSRs prefers at more than **7 sigma** the contribution of both a disk AND an inner Galaxy populations.
- **The best fit for the number of PSRs in the disk and the inner Galaxy and its spatial distribution is perfectly consistent with the 3FGL PSRs and curved sources and with the GC excess properties.**
- A definitive confirmation of this interpretation will come from the detection of radio pulsation from many of these candidates (SKA-mid-like survey will be able to find dozens of PSRs).

BACKUP SLIDES

Prospects for detection of PSR from the Galactic bulge in radio (Calore et al. 2016)

- Definitive confirmation that these sources are in fact pulsars will require detection of pulsations in radio or γ-ray for several of the sources.
- We investigated the prospects for detection with current radio telescopes.
- Parkes or the Green Bank Telescope can achieve the detection of a few PSRs from the bulge.
- SKA-mid-like survey will be able to find dozens of PSRs.

SKA

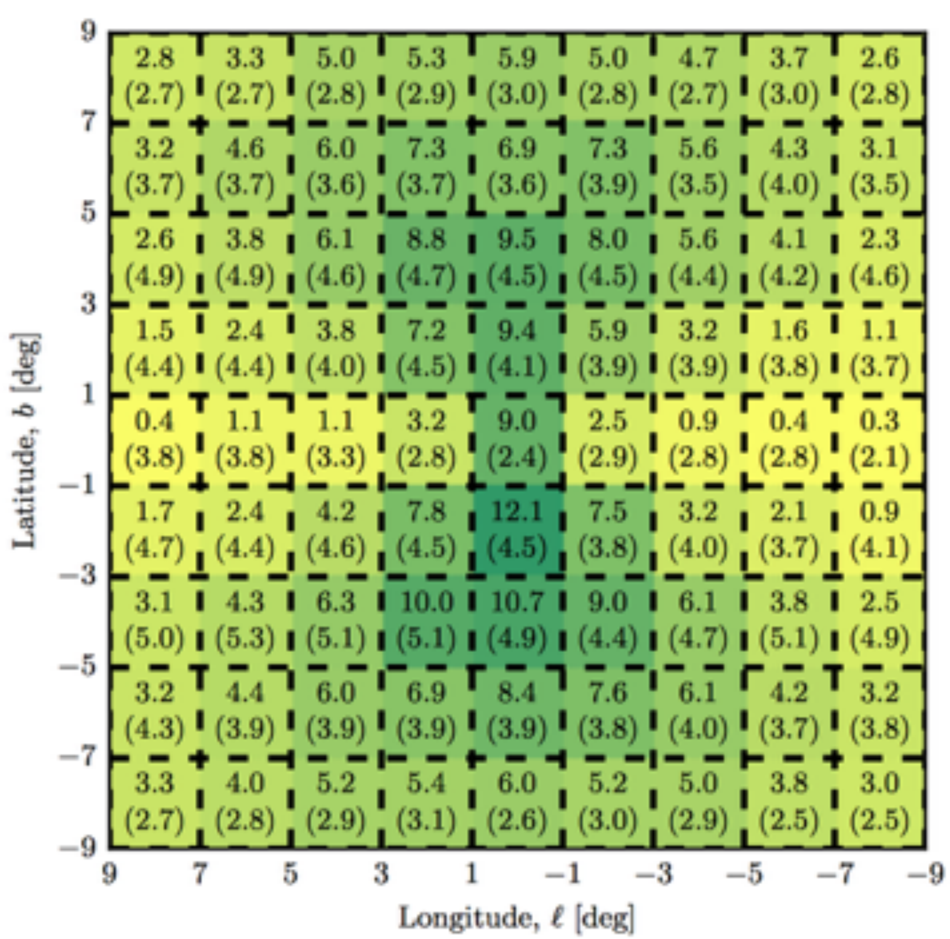

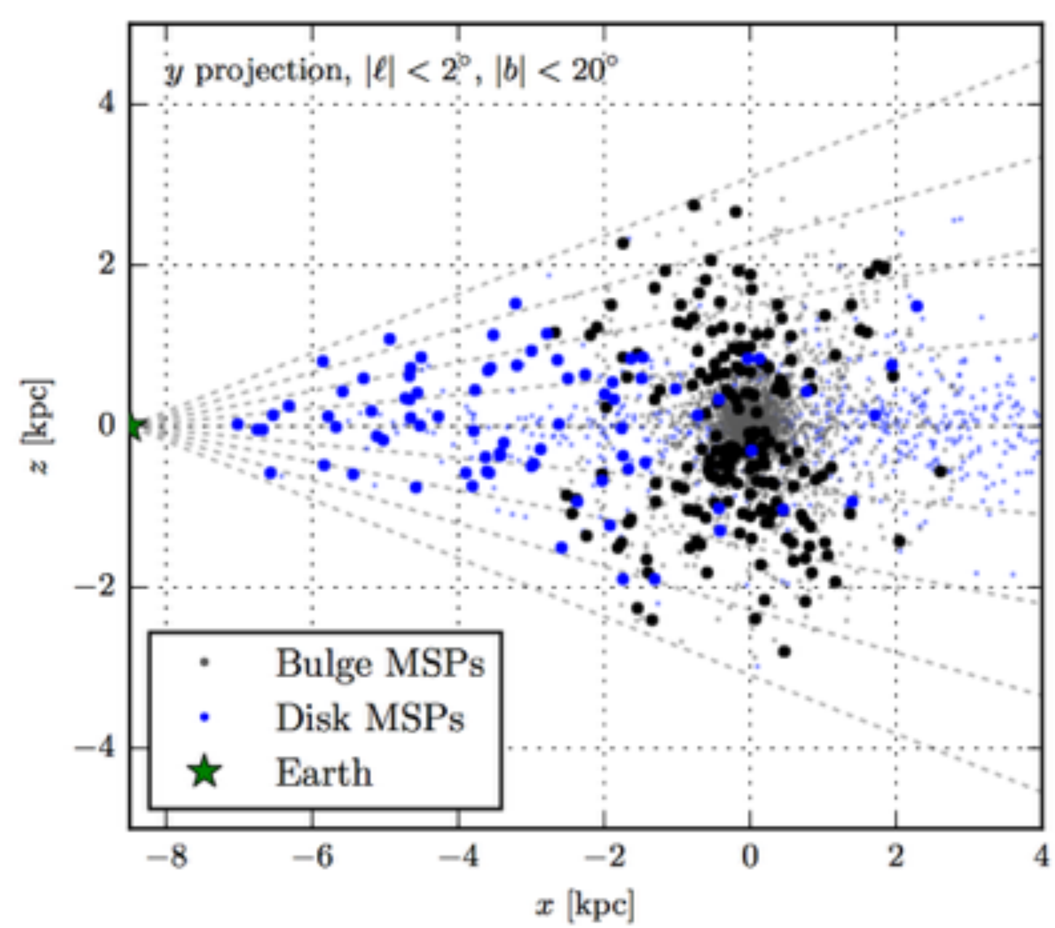

Calore et al. 2016

Efficiency for the detection of PSR candidates

- We tabulated the efficiency for bins in longitude, latitude and energy flux: **ω(l,b,S)**
- We make 10 simulations of PSRs distributed in the Galaxy according to an inner Galaxy and an isotropic distribution of PSRs.
- We analyze the simulations with the same tools we use for the real sky and we select sources with **TS^{PLE}_{curv}>9, Index<2.0 and E_{cut}<10GeV.**
- (We simulate sources from Γ=1.33±0.54 and Log10(E_{cut})=3.43±0.24 and the detected PSR candidates have **Γ=1.11±0.60 and Log10(E_{cut})=3.37±0.24.)**

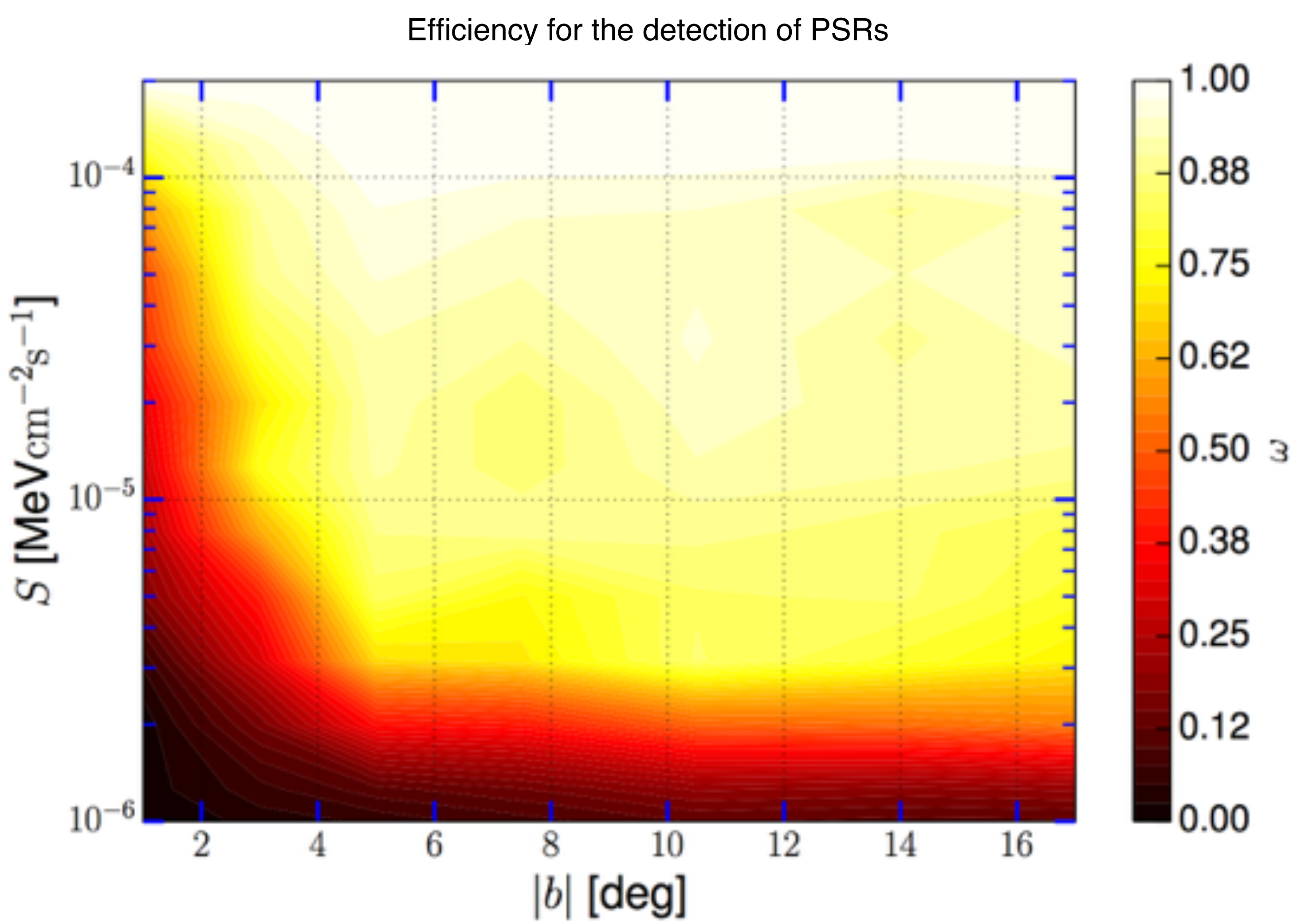

Prior on the number of bright PSRs

- We introduce in the MLA a prior to reproduce the number of bright PSRs already detected by the LAT.
- **Lower Limit:** number of PSRs already identified.
- **Upper limit:** γ-ray PSRs already detected + Unassociated 3FGL sources with a curved SED.

$$\mathcal{L}_{\text{prior}} = \frac{(N^{\text{model}}_{S>S_0}(\lambda) - N^{\text{data}}_{S>S_0})^2}{2{\sigma_N}^2}$$

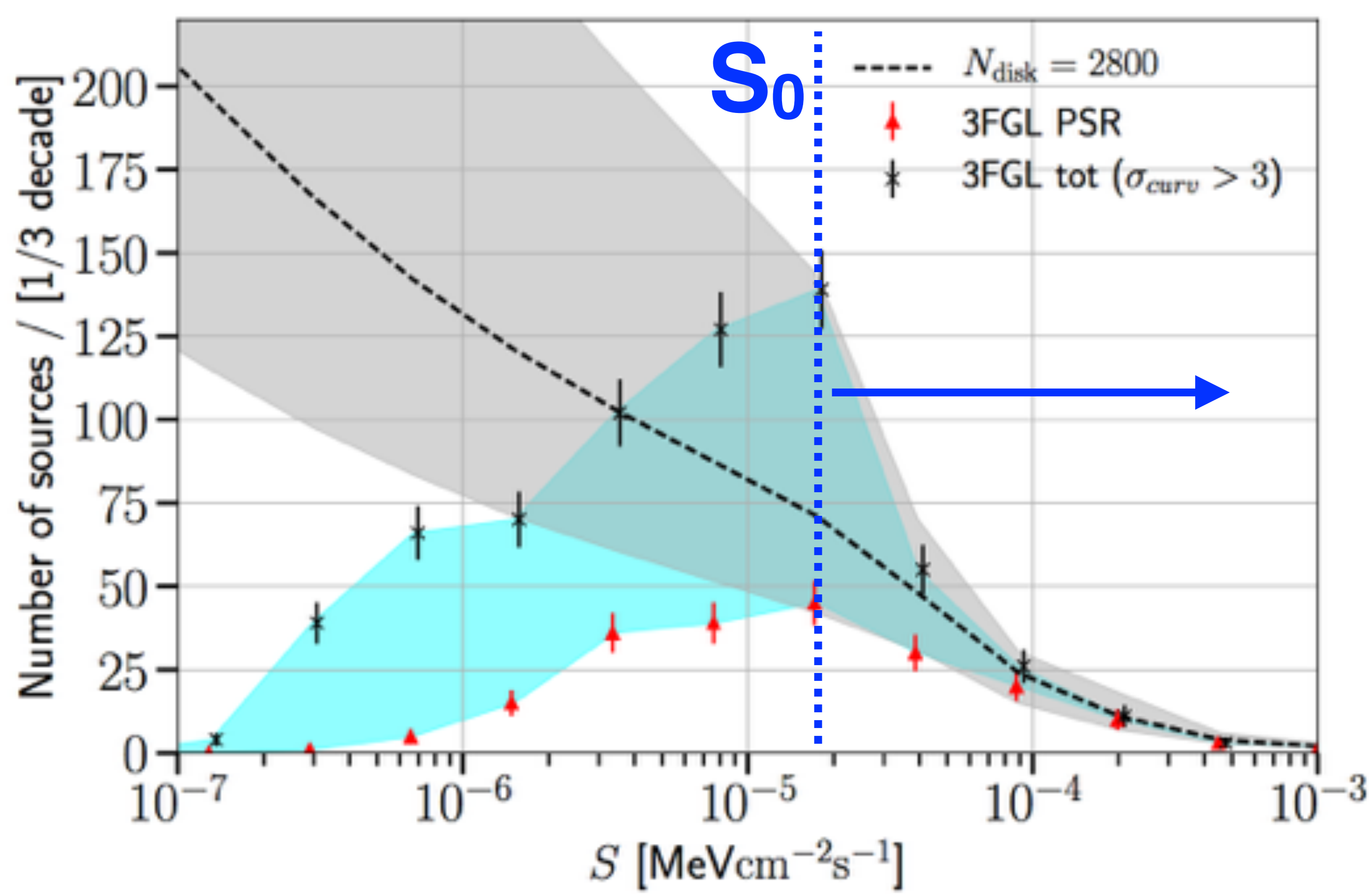

Results for the disk+bulge populations

3.3deg bin

	Alternate IEM						Official IEM					
A	$N_{\rm disk}$	z_0[kpc]	β	$N_{\rm bulge}$	α	TS	$N_{\rm disk}$	z_0[kpc]	β	$N_{\rm bulge}$	α	TS
1	23500^{+5500}_{-5000}	$0.63^{+0.14}_{-0.14}$	$1.35^{+0.07}_{-0.07}$	0	$\cdots$	0	22500^{+5200}_{-4800}	$0.71^{+0.16}_{-0.16}$	$1.34^{+0.07}_{-0.07}$	0	$\cdots$	0
2	3740^{+1030}_{-940}	$0.66^{+0.14}_{-0.14}$	$1.23^{+0.06}_{-0.06}$	1580^{+330}_{-270}	2.60	60	3560^{+980}_{-870}	$0.72^{+0.17}_{-0.17}$	$1.24^{+0.06}_{-0.06}$	1330^{+270}_{-210}	2.60	63
3	3960^{+1070}_{-970}	$0.70^{+0.16}_{-0.16}$	$1.24^{+0.07}_{-0.07}$	1660^{+350}_{-300}	$2.55^{+0.24}_{-0.24}$	65	3610^{+1010}_{-930}	$0.75^{+0.18}_{-0.18}$	$1.25^{+0.07}_{-0.07}$	1370^{+280}_{-220}	$2.57^{+0.23}_{-0.23}$	69
B	$N_{\rm disk}$	z_0[kpc]	β	$N_{\rm bulge}$	α	TS	$N_{\rm disk}$	z_0[kpc]	β	$N_{\rm bulge}$	α	TS
1	25600^{+5900}_{-5200}	$0.72^{+0.22}_{-0.22}$	$1.37^{+0.13}_{-0.13}$	0	$\cdots$	0	24500^{+5700}_{-5000}	$0.76^{+0.23}_{-0.23}$	$1.33^{+0.14}_{-0.14}$	0	$\cdots$	0
2	4670^{+1350}_{-1230}	$0.69^{+0.21}_{-0.21}$	$1.25^{+0.12}_{-0.12}$	1380^{+370}_{-310}	2.60	53	3710^{+1270}_{-1150}	$0.75^{+0.23}_{-0.23}$	$1.26^{+0.12}_{-0.12}$	1310^{+350}_{-290}	2.60	54
3	4360^{+1370}_{-1180}	$0.68^{+0.20}_{-0.20}$	$1.24^{+0.11}_{-0.11}$	1430^{+380}_{-320}	$2.57^{+0.27}_{-0.27}$	58	3660^{+1210}_{-1110}	$0.73^{+0.22}_{-0.22}$	$1.25^{+0.12}_{-0.12}$	1350^{+330}_{-300}	$2.65^{+0.28}_{-0.28}$	59

6deg bin

Latitude Profile of Bulge Sources

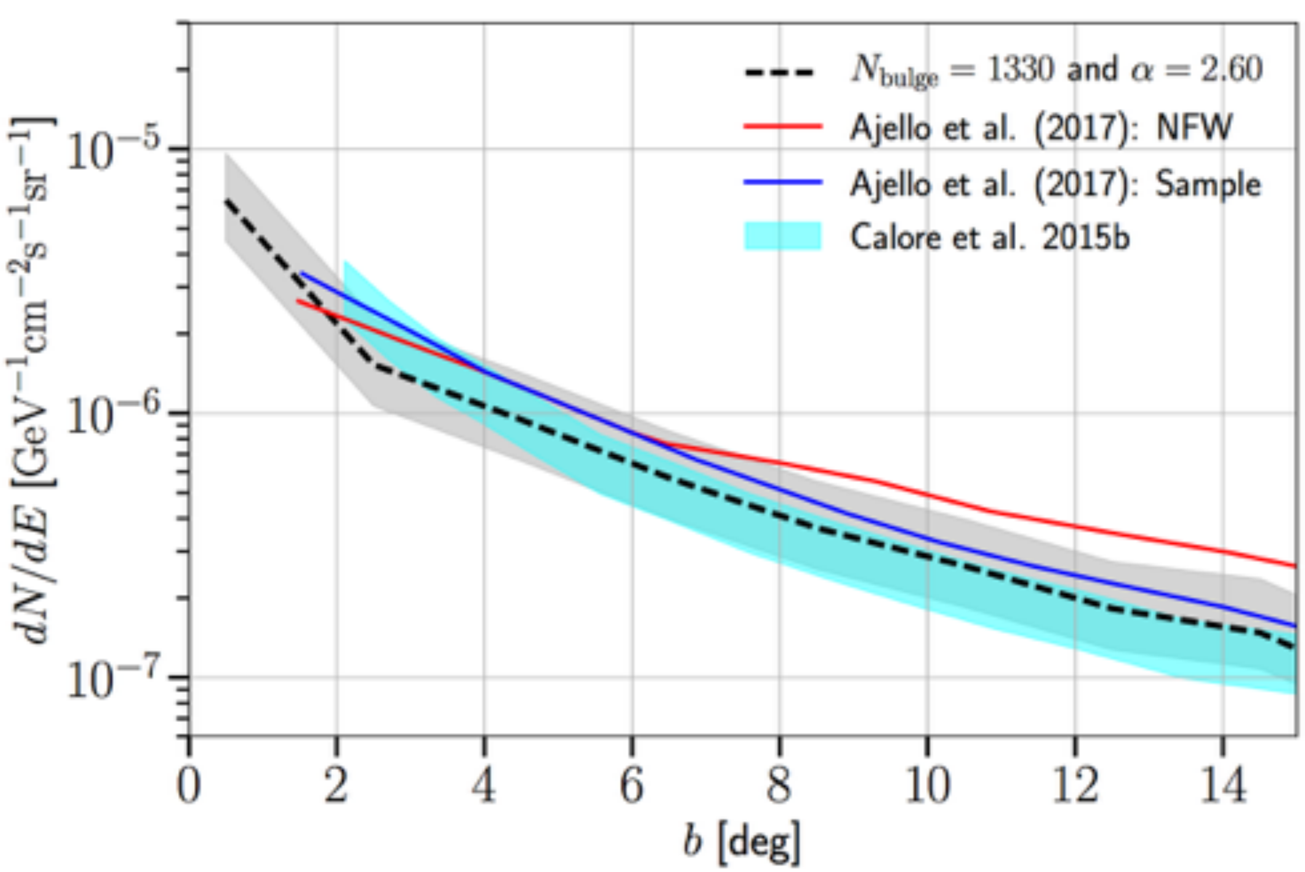

SED of Bulge Sources

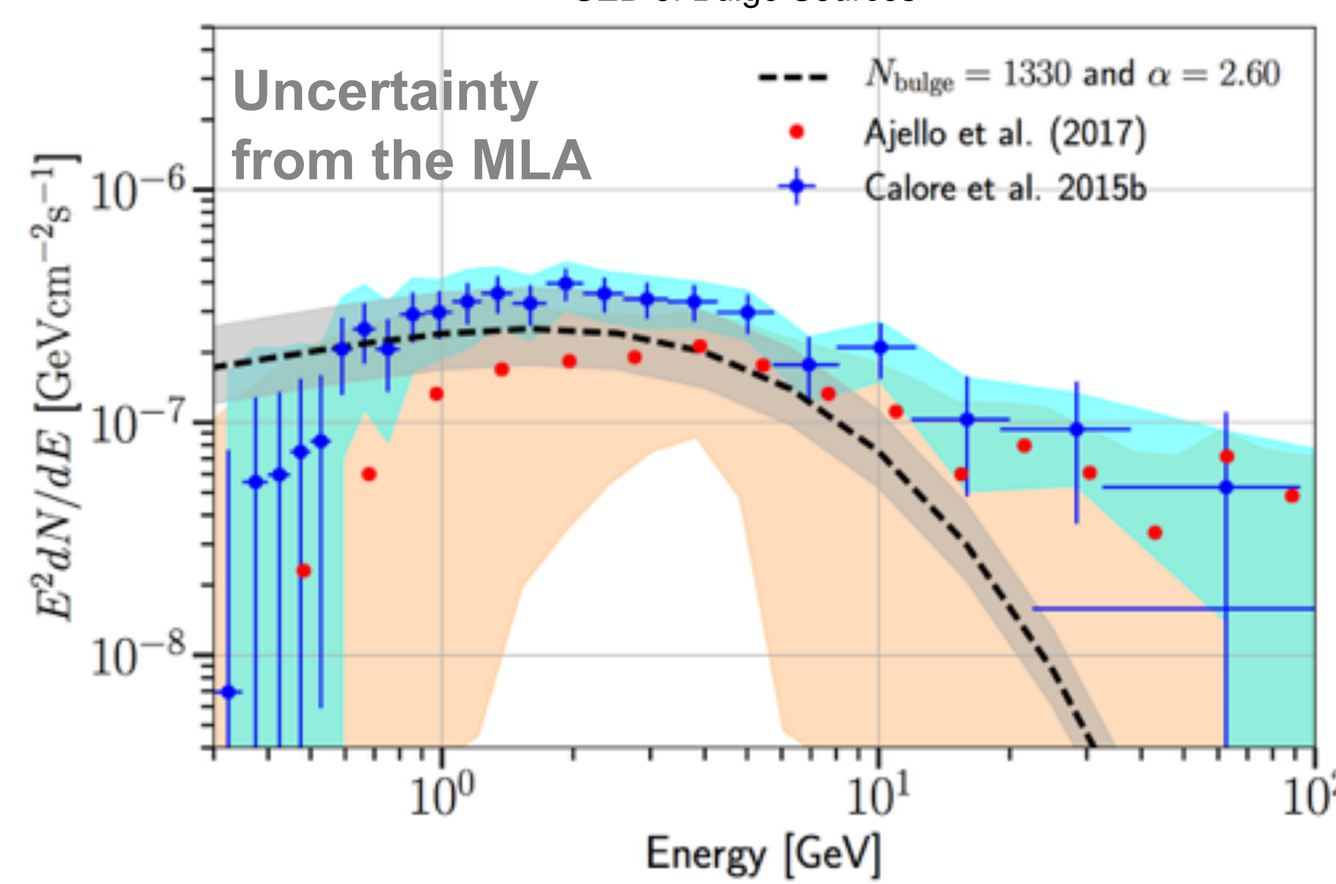

arXiv:1611.01015 (recently accepted in ApJ)

THE EINSTEIN@HOME GAMMA-RAY PULSAR SURVEY I: SEARCH METHODS, SENSITIVITY AND DISCOVERY OF NEW YOUNG GAMMA-RAY PULSARS

C. J. Clark[1,2,3], J. Wu[4], H. J. Pletsch[1,2], L. Guillemot[5,6,4], B. Allen[1,7,2], C. Aulbert[1,2], C. Beer[1,2], O. Bock[1,2], A. Cuéllar[1,2], H. B. Eggenstein[1,2], H. Fehrmann[1,2], M. Kramer[8,4], B. Machenschalk[1,2], and L. Nieder[1,2]

Table 4. Derived pulsar properties

Pulsar	l (°)	b (°)	P (ms)	$\dot{P}$ (10^{-15} s s^{-1})	τ_c (kyr)	$\dot{E}$ (10^{33} erg s^{-1})	B_S (10^{12} G)
J0002+6216	117.33	−0.07	115.363568268(2)	5.96703(7)	306	153	0.8
J0359+5414	148.23	+0.88	79.427232292(1)	16.73359(7)	75	1318	1.2
J0631+0646	204.68	−1.24	110.9789432160(7)	3.61723(2)	486	104	0.6
J1057−5851	288.61	+0.80	620.3650313(1)	100.583(5)	98	17	8.0
J1105−6037	290.24	−0.40	194.938267113(3)	21.83720(6)	141	116	2.1
J1350−6225	309.73	−0.34	138.157778213(1)	8.88352(4)	246	133	1.1
J1528−5838	322.17	−1.75	355.686622097(8)	24.7586(2)	228	22	3.0
J1623−5005	333.72	−0.31	85.0721461635(8)	4.16118(2)	324	267	0.6
J1624−4041	340.56	+6.15	167.861145148(1)	4.72489(2)	563	39	0.9
J1650−4601	339.78	−0.95	127.122893310(2)	15.14468(6)	133	291	1.4
J1827−1446	17.08	−1.50	499.18661037(3)	45.3351(9)	174	14	4.8
J1844−0346	28.79	−0.19	112.85464991(1)	154.7031(6)	12	4249	4.2
J2017+3625	74.51	+0.39	166.7491790419(8)	1.35985(2)	1943	12	0.5